

Scattering of charge and spin excitations and equilibration of a one-dimensional Wigner crystal

K. A. Matveev,¹ A. V. Andreev,² and A. D. Klironomos³

¹*Materials Science Division, Argonne National Laboratory, Argonne, Illinois 60439, USA*

²*Department of Physics, University of Washington, Seattle, Washington 98195, USA*

³*American Physical Society, 1 Research Road, Ridge, New York 11961-9000*

(Dated: July 28, 2014)

We study scattering of charge and spin excitations in a system of interacting electrons in one dimension. At low densities electrons form a one-dimensional Wigner crystal. To a first approximation the charge excitations are the phonons in the Wigner crystal, and the spin excitations are described by the Heisenberg model with nearest neighbor exchange coupling. This model is integrable and thus incapable of describing some important phenomena, such as scattering of excitations off each other and the resulting equilibration of the system. We obtain the leading corrections to this model, including charge-spin coupling and the next-nearest neighbor exchange in the spin subsystem. We apply the results to the problem of equilibration of the one-dimensional Wigner crystal and find that the leading contribution to the equilibration rate arises from scattering of spin excitations off each other. We discuss the implications of our results for the conductance of quantum wires at low electron densities.

PACS numbers: 71.10.Pm

I. INTRODUCTION

The low-energy properties of one-dimensional electron systems are commonly described in the framework of the Tomonaga-Luttinger liquid theory.¹ In this approach the electrons are described in terms of elementary excitations with bosonic statistics, which have the meaning of waves of charge and spin densities. These waves propagate at different velocities,² resulting in the separation of the charge and spin of the electrons. A detailed theory of spin-charge separation can be developed in the case of strong repulsive interactions. This was first accomplished for the one-dimensional Hubbard model by Ogata and Shiba,³ who showed that the ground state wave function of the system can be expressed as a product of two separate wave functions describing the charge and spin degrees of freedom.

Experimentally, one-dimensional electron systems are often realized in GaAs quantum wires.⁴ In contrast to the Hubbard model, electrons in quantum wires are not confined to discrete lattice sites, and interact via the long-range Coulomb repulsion $V(x) = e^2/\epsilon|x|$. The density of electrons in these systems is easily controlled by gates. At low density $n \ll a_B^{-1}$ the Coulomb repulsion between electrons is much larger than their kinetic energy, and in the ground state the system forms a Wigner crystal.⁵ (Here $a_B = \epsilon\hbar^2/me^2$ is the Bohr radius in the material, ϵ is the dielectric constant, and m is the effective mass of the electrons.)

This physical picture of strongly interacting one-dimensional electron systems enables a simple description of the charge excitations as phonons in the Wigner crystal. Mathematically, they are accounted for by the

phonon Hamiltonian

$$H_p^{(0)} = \sum_l \frac{p_l^2}{2m} + \frac{e^2}{2\epsilon a^3} \sum_{l \neq l'} \frac{(u_l - u_{l'})^2}{|l - l'|^3}, \quad (1)$$

where $a = n^{-1}$ is the average interelectron distance, and the l th electron is described by its momentum p_l and displacement from the equilibrium position $u_l = x_l - la$.

As long as the displacements u_l are small, the spins are attached to the lattice sites. In order for the spins to move along the crystal, neighboring electrons must be able to switch places on the Wigner lattice. Such processes lead to the exchange coupling of the spins⁶

$$H_s^{(0)} = \sum_l J \mathbf{S}_l \cdot \mathbf{S}_{l+1}. \quad (2)$$

Because the exchange process involves two adjacent electrons tunneling through the strong Coulomb barrier $e^2/\epsilon|x_l - x_{l+1}|$, the coupling constant J is exponentially small

$$J \sim (na_B)^{5/4} \frac{e^2}{\epsilon a_B} \exp\left(-\frac{\eta}{\sqrt{na_B}}\right), \quad (3)$$

where $\eta \approx 2.798$.⁶⁻⁸

The Hamiltonian given by Eqs. (1) and (2) describes the charge and spin excitations in the Wigner crystal near the ground state. At finite temperature the electron density fluctuates, resulting in thermal fluctuations of the exchange constant (3). This limits the applicability of the Hamiltonian (1) and (2) to relatively low temperatures, $T \ll (e^2/\epsilon a_B)(na_B)^{7/4}$. Note that this range includes the most interesting temperature regime $T \lesssim J$.

As expected, the charge and spin fluctuations described by Eqs. (1) and (2) are decoupled from each other. Another interesting feature of this Hamiltonian

is its integrability. Indeed, Eq. (1) describes noninteracting phonons, and integrability of the spin- $\frac{1}{2}$ Heisenberg model (2) was shown by Bethe⁹ in 1931. A defining characteristic of integrable models is a large number of integrals of motion, which prevents relaxation of the system to equilibrium. Thus, although the Hamiltonian (1), (2) gives an adequate description of the equilibrium properties of the system, corrections to it must be considered in order to discuss the approach to equilibrium. Examples of physical effects controlled by equilibration include various transport phenomena in high-mobility quantum wires.^{10–16}

The first goal of this paper is to identify and evaluate the leading order corrections to the Hamiltonian (1), (2). Such corrections fall into three categories. First, one should note that the Wigner crystal is not a perfectly harmonic chain. Anharmonic corrections to the Hamiltonian (1) are determined by the third and higher derivatives of the interaction potential and are well understood. Corrections of the second type account for coupling between the charge and spin excitations. They can be understood by noting that the exchange constant J in Eq. (2) depends on the electron density, Eq. (3), which fluctuates as the phonons propagate through the system. Corrections of the third type appear in the spin channel. Similarly to the nearest neighbor exchange coupling (2), they are caused by quantum tunneling processes resulting in some electrons changing places on the Wigner lattice.

Our second goal is to develop a theory of equilibration of a one-dimensional Wigner crystal at the lowest temperatures $T \ll J$. The full equilibration of one-dimensional systems is an exponentially slow process, as it requires backscattering of highly excited hole quasiparticles.^{10,17–19} In the case of strong interactions the hole becomes a spinon excitation in the spin chain formed on the lattice sites of the Wigner crystal, see Eq. (2). Because the typical energy of the spinon J is small compared to the Fermi energy, the equilibration rate is greatly enhanced in this regime. It is dominated by the processes of scattering of spinons by the thermal excitations of the system. The evaluation of the scattering rate relies heavily on the preceding results for the form and magnitude of the integrability-breaking perturbations in the one-dimensional Wigner crystal.

We discuss the corrections to the Hamiltonian (1), (2) in Sec. II. The study of the exchange processes beyond the nearest neighbor coupling requires the calculation of the relevant tunneling amplitudes in the WKB approximation. We evaluate the WKB action for the dominant three-particle exchange process in Sec. III. In addition to corrections to the nearest neighbor exchange constant (3), this process generates exchange coupling of the next nearest neighbor spins in the crystal, which breaks the integrability of the Heisenberg chain. In Sec. IV we use the results of Secs. II and III to evaluate the rate of full equilibration of the Wigner crystal at low temperatures. In Sec. V we summarize our results and discuss their impli-

cations for the temperature dependence of conductance of quantum wires.

II. HAMILTONIAN OF THE WIGNER CRYSTAL

One-dimensional electrons interacting via sufficiently strong repulsion form a periodic chain regardless of the spatial dependence of the interaction potential $V(x)$, except for an extremely short-ranged interaction. In this paper we focus on the case of pure Coulomb repulsion $V(x) = e^2/\varepsilon|x|$, corresponding to the traditional definition of the Wigner crystal. The regime of strong repulsion is realized at low electron density n , when the typical energy of Coulomb repulsion $(e^2/\varepsilon)n$ greatly exceeds the typical kinetic energy $(\hbar^2/m)n^2$ in a free electron gas. Thus the Wigner crystal limit is achieved at $na_B \ll 1$, or at

$$r_s = \frac{1}{2na_B} \gg 1. \quad (4)$$

It is worth mentioning that in one dimension quantum fluctuations destroy long-range order even at zero temperature, and the Wigner crystal picture refers only to the short-range ordering of electrons.

The full microscopic Hamiltonian of one-dimensional electrons with Coulomb interactions is given by

$$H = \sum_l \frac{p_l^2}{2m} + \frac{1}{2} \sum_{l \neq l'} \frac{e^2}{\varepsilon|x_l - x_{l'}|}. \quad (5)$$

Our goal in this section is to develop the low energy description of the system at $na_B \ll 1$.

A. Spin-charge separation

To leading order in na_B , electrons do not switch places on the Wigner lattice. Indeed, in order to do so one-dimensional electrons must approach each other and experience strong Coulomb repulsion. As a result, this process is essentially tunneling under the Coulomb barrier,³⁶ and its amplitude is exponentially small. As long as electrons do not switch places, their spins do not interact, and each state of N particles is 2^N -fold degenerate.

The effect of the tunneling processes can be understood as follows. Because the Hamiltonian (5) does not depend on spins, the eigenstates of the system factorize into the product of the coordinate and spin components:

$$\psi(x_1, \sigma_1; \dots; x_N, \sigma_N) = \chi_{\sigma_1, \dots, \sigma_N} \phi(x_1, \dots, x_N). \quad (6)$$

The coordinate wavefunction $\phi(x_1, \dots, x_N)$ satisfies

$$H\phi = E\phi \quad (7)$$

with H given by Eq. (5). One can interpret Eq. (7) as the Schrödinger equation for a system of N spinless distinguishable particles. In the absence of tunneling the

spatial ordering of the particles is preserved. Furthermore, for any state $\phi(x_1, \dots, x_N)$, there are a total of $N!$ degenerate states obtained from it by all permutations of the coordinates x_1, \dots, x_N . The strongest tunneling process permutes two adjacent particles. Thus, at low energies, the Hamiltonian (5) can be approximated as

$$H = H_\rho - \frac{J}{2} \sum_l P(x_l, x_{l+1}), \quad (8)$$

where $P(x_i, x_j)$ is the operator of the permutation of the coordinates of the i th and j th particles. The constant J can be computed in the WKB approximation⁶⁻⁸ and is given by Eq. (3).

The operator H_ρ in Eq. (8) coincides with Eq. (5) with the additional condition that no switching of the position of the particles is allowed. It can be formally defined by adding to Eq. (5) the point-like repulsive potential $A\delta(x_l - x_{l'})$ with $A \rightarrow +\infty$. In the Wigner crystal approximation one expresses the coordinates of the particles in terms of their displacements from lattice sites, $x_l = la + u_l$. Expanding the interaction term to second order in u_l one obtains the phonon Hamiltonian (1).

When applying the result (8) to a system of identical fermions one should bear in mind that the wavefunction (6) changes sign upon simultaneous permutation of coordinates $x_l \leftrightarrow x_{l+1}$ and spins $\sigma_l \leftrightarrow \sigma_{l+1}$. Thus for fermions the two permutations are related as $P(x_l, x_{l+1}) = -P_{\sigma_l, \sigma_{l+1}}$, where

$$P_{\sigma_i, \sigma_j} = \frac{1}{2} + 2\mathbf{S}_i \cdot \mathbf{S}_j \quad (9)$$

is the operator of permutation of spins i and j . Using this result we find that the second term in Eq. (8) gives the spin Hamiltonian (2).

Equations (1) and (2) represent the leading contributions to the low-energy Hamiltonian of the system. As discussed above, the resulting theory is integrable, which precludes scattering of either charge or spin excitations. The latter is made possible by the subleading contributions to the Hamiltonian. They include corrections in the charge sector, in the spin sector, and the coupling between the charge and spin sectors.

B. Charge sector

It is convenient to rewrite Eq. (1) in terms of the phonon operators b_q, b_q^\dagger using the standard relations

$$u_l = \sum_q \sqrt{\frac{\hbar}{2mN\omega_q}} (b_q + b_{-q}^\dagger) e^{iql}, \quad (10)$$

$$p_l = -i \sum_q \sqrt{\frac{\hbar m \omega_q}{2N}} (b_q - b_{-q}^\dagger) e^{iql}. \quad (11)$$

Here $N = nL$ is the total number of electrons in a system of size L , and the phonon frequencies are found by solving

the classical equations of motion with the Hamiltonian (1),

$$\hbar\omega_q = 2(na_B)^{3/2} \frac{e^2}{\varepsilon a_B} \left[\sum_{l=1}^{\infty} \frac{1 - \cos(ql)}{l^3} \right]^{1/2}. \quad (12)$$

This yields

$$H_\rho^{(0)} = \sum_q \hbar\omega_q \left(b_q^\dagger b_q + \frac{1}{2} \right). \quad (13)$$

The behavior of ω_q at $q \rightarrow 0$ is discussed in Appendix A.

Beyond the harmonic approximation, one finds corrections to the Hamiltonian (13), which include terms of third and higher powers in the phonon operators b_q and b_q^\dagger and can be interpreted as interactions of the phonons. Expanding the Coulomb interaction in Eq. (5) to all orders in electron displacements, one can express the anharmonic corrections to $H_\rho^{(0)}$ as

$$H_\rho = H_\rho^{(0)} + \sum_{r=3}^{\infty} \hat{V}_\rho^{(r)}, \quad (14)$$

$$\hat{V}_\rho^{(r)} = \frac{e^2}{\varepsilon a^{r+1}} \sum_{l>l'} \frac{(u_{l'} - u_l)^r}{(l - l')^{r+1}}. \quad (15)$$

This expression can be equivalently written in terms of the phonon operators using Eq. (10).

C. Spin sector

The Hamiltonian (2) accounts for the processes of two nearest neighbor electrons switching positions on the Wigner lattice. Additional contributions to the spin Hamiltonian will appear from any cyclic exchange process, including exchanges of two next-nearest neighbors, three consecutive electrons, four consecutive electrons, etc. The four processes we listed were considered in the case of a quasi-one-dimensional Wigner crystal.^{20,21} The range of electron densities considered there was above the transition from a purely one-dimensional Wigner crystal into the zigzag phase. Based on the results of Refs. 20 and 21 in the region of lowest densities studied, where the zigzag distortion is small, we conclude that the strongest exchange is that of nearest neighbors, and the next strongest one involves three consecutive electrons.

One can account for the three-particle exchange processes following the prescription of Sec. II A. In addition to the two-particle exchange term in Eq. (8) one obtains the contribution of the form

$$-\frac{\tilde{J}}{2} \sum_l [P(x_l, x_{l+1}, x_{l+2}) + P(x_l, x_{l+2}, x_{l+1})], \quad (16)$$

where the operator $P(x_i, x_j, x_k)$ performs a cyclic permutation of coordinates $x_i \rightarrow x_j \rightarrow x_k \rightarrow x_i$. Because

this is an even permutation, its outcome is equivalent to the permutation of electron spins $P_{\sigma_i, \sigma_k, \sigma_j}$. One can therefore rewrite the perturbation (16) as

$$-\frac{\tilde{J}}{2} \sum_l [P_{\sigma_l, \sigma_{l+1}, \sigma_{l+2}} + P_{\sigma_l, \sigma_{l+2}, \sigma_{l+1}}] \\ = -\tilde{J} \sum_l \left[\frac{1}{4} + \mathbf{S}_l \cdot \mathbf{S}_{l+1} + \mathbf{S}_{l+1} \cdot \mathbf{S}_{l+2} + \mathbf{S}_l \cdot \mathbf{S}_{l+2} \right],$$

where we used the expression for the three-spin permutation in terms of the spin operators obtained in Ref. 22. Omitting the inessential constant, we get the following perturbation in the spin Hamiltonian due to the exchange of three consecutive electrons

$$\hat{V}_\sigma = - \sum_l \tilde{J} [2 \mathbf{S}_l \cdot \mathbf{S}_{l+1} + \mathbf{S}_l \cdot \mathbf{S}_{l+2}]. \quad (17)$$

The constant \tilde{J} will be evaluated in the WKB approximation in Sec. III. We will see that \tilde{J} is exponentially smaller than the nearest neighbor exchange constant J . Thus the first term in the right-hand side of Eq. (17) gives only a negligible correction to J . On the other hand, the second term couples next nearest neighbor spins. Such perturbations break integrability of the Heisenberg model (2) and give rise to relaxation of spin excitations.

D. Spin-charge coupling

So far we discussed corrections to the low-energy Hamiltonian of the Wigner crystal given by Eqs. (1) and (2), which give rise to the scattering of excitations separately in the charge and spin sectors. As a result of such scattering the excitations equilibrate within each sector, but not with the excitations in the other sector. Full equilibration of the system requires coupling of the charge and spin excitations, which we discuss below.

The magnitude of the exchange constant J depends strongly on the electron density [see Eq. (3)]. The latter varies when phonons propagate through the system, giving rise to the coupling of the charge and spin degrees of freedom.²² One can account for this effect by evaluating J in Eq. (2), using instead of the average density n in Eq. (3) the position-dependent electron density in the presence of the phonon deformation:

$$n \rightarrow \frac{1}{a + u_{l+1} - u_l} = \frac{n}{1 + n(u_{l+1} - u_l)}. \quad (18)$$

To lowest order in the phonon displacements and na_B , this procedure results in the coupling of the charge and spin degrees of freedom in the form

$$\hat{V}_{\rho\sigma} = -J \frac{\eta}{2\sqrt{na_B}} \sum_l n(u_{l+1} - u_l) \mathbf{S}_l \cdot \mathbf{S}_{l+1}. \quad (19)$$

The displacements u_l in (19) can be expressed in terms of the phonon operators using Eq. (10). The above procedure is justified as long as the phonon density fluctuations

remain approximately uniform at the scale of interparticle distance, i.e., for phonons with $|q| \ll 1$. The same condition ensures that the density fluctuations are static on the scale of the WKB tunneling time.

III. THREE-PARTICLE EXCHANGE IN THE WKB APPROXIMATION

Spin exchange in the Wigner crystal is caused by quantum tunneling processes which allow electrons to switch places on the Wigner lattice. We discussed these exchange processes in Secs. II A and II C. In particular, we found the expression (17) for the leading order correction to the spin Hamiltonian (2). In this section we discuss the magnitude of the respective exchange constant \tilde{J} .

At small na_B , the tunneling amplitudes are small and can be evaluated in the WKB approximation. We perform the calculation using the instanton technique. In this approach the tunneling amplitudes are controlled by the imaginary-time action

$$S[\{x_l(t)\}] = \int \left(\sum_l \frac{m}{2} \dot{x}_l^2 + \sum_{l < l'} \frac{e^2}{\varepsilon |x_l - x_{l'}|} \right) dt. \quad (20)$$

It is convenient to introduce the dimensionless coordinates X_l and time τ as

$$x_l = \frac{1}{n} X_l, \quad t = \frac{\hbar \varepsilon a_B}{(na_B)^{3/2} e^2} \tau. \quad (21)$$

This procedure brings Eq. (20) to the form

$$\frac{1}{\hbar} S[\{x_l(t)\}] = \frac{1}{\sqrt{na_B}} \eta[\{X_l(\tau)\}], \quad (22)$$

where η is the dimensionless action

$$\eta[\{X_l(\tau)\}] = \int \left(\sum_l \frac{1}{2} \dot{X}_l^2 + \sum_{l < l'} \frac{1}{|X_l - X_{l'}|} \right) d\tau. \quad (23)$$

It is minimized for the trivial trajectory $X_l(\tau) = l$.

The cyclic exchange of three particles in Eq. (16) is described by trajectories with boundary conditions $X_l = l$ at $\tau \rightarrow -\infty$ and

$$X_0 = 2, \quad X_1 = 0, \quad X_2 = 1; \quad X_l = l, \quad l \neq 0, 1, 2 \quad (24)$$

at $t \rightarrow +\infty$. In the WKB approximation, the coupling constant \tilde{J} is given by

$$\tilde{J} = \tilde{J}^* \exp \left(-\frac{\tilde{\eta}}{\sqrt{na_B}} \right), \quad (25)$$

where $\tilde{\eta}$ is the difference between the minimum action of the cyclic exchange trajectory and the action of the trivial trajectory $X_l(\tau) = l$. We evaluate the instanton action and obtain $\tilde{\eta}$ numerically in Sec. III A. The preexponential factor \tilde{J}^* is discussed in Sec. III B.

A. Numerical evaluation of the instanton action

The full consideration of any exchange of particles in the Wigner crystal requires that the motion of all particles forming the crystal is taken into account. In practice, the consideration of a large number of them is feasible. Assuming that in addition to n particles exchanging positions, N spectators ($N/2$ on each side of the exchanging cluster) are free to move from their equilibrium positions, the numerical minimization of the dimensionless action Eq. (23) over the particle trajectories $X_l(\tau)$ is straightforward to set up. The case of a single instanton where two adjacent particles exchange positions has been examined in detail previously.⁷ In general, the problem is equivalent to solving a system of $n + N$ second-order differential equations of motion with appropriate boundary conditions reflecting the initial and final state of the system.

We take the opportunity here to introduce a shorthand notation for relevant exchanges, denoting them by the index at static equilibrium of the particles involved. For example, [01] stands for the two-particle exchange involving electrons labeled by $l = 0$ and 1. Multiple exchanges can be chained together as we will see below.

One complication is the divergence of the bare Coulomb interaction and the treatment of the associated singularity when two particles occupy the same position in the course of the exchange. There are various well-documented methods of how to treat such singularities in order to obtain the solutions to the corresponding differential equations of motion. It is simpler and better suited for our purposes to consider a regularized Coulomb interaction by introducing a small cutoff δ :

$$\frac{1}{|X_l - X_{l'}|} \rightarrow \frac{1}{|X_l - X_{l'}| + \delta}, \quad (26)$$

and study the evolution of the solutions as $\delta \rightarrow 0$.

Considering two interacting instantons brings additional complications in the calculation which will be explained below. Starting with the simplest nontrivial exchange beyond nearest-neighbor, one has to consider the exchange of three particles which is illustrated in panel (a) of Fig. 1. Following the convention adopted above we call it [01–12] for the sake of brevity.

At sufficiently large temporal distance τ_0 between the two interacting instantons, the calculation is equivalent to that of two single instantons, resulting in an exponent two times that of the single instanton: $\eta_\infty = 2\eta$; see Appendix B for a more detailed exposition. At this stage, the minimization of the dimensionless action Eq. (23), i.e. the solution of the differential equations of motion, is carried out at fixed distance τ_0 , by splitting the imaginary time interval into appropriate pieces and joining the solutions using standard methods.

By examining the action as τ_0 is varied, we find that the instantons attract at large distances and repel at short distances. The system permits an intuitive electrostatic analogy in terms of interacting dipoles, which is

further developed in Appendix B [see Eq. (B10)]. Bringing the instantons closer together, we discover that their interaction has a minimum at a temporal distance τ_0 of the order of the temporal extent of the instanton. That characteristic distance τ_0 depends on the number of spectators that are allowed to move in addition to the exchanging triad. As a result, the distance between the instantons becomes an additional minimization parameter for the numerical treatment of this problem. Therefore, the full calculation consists of a minimization with respect to τ_0 on top of each minimization of the dimensionless action Eq. (23).

Similar considerations apply for the more complicated exchanges shown in panels (b) and (c) of Fig. 1. Among a large set of possible candidates, these are the ones that are intuitively most relevant. Detailed calculations confirm that they are negligible compared to the contribution of [01–12].

Figure 2 shows how the difference $\Delta\eta = \eta_{min} - \eta_\infty$ between the exponent corresponding to infinite distance τ_0 between the instantons and that obtained at the minimum depends on the number of spectators and the cutoff used in the calculations. A cutoff $\delta = 10^{-3}$ is more than adequate for this comparison, and it in fact gives an excellent approximation to the result one would obtain with an unscreened Coulomb interaction for [01–23] and [01–34]. Given the considerable separation between the curves, it is reasonable to claim that even at the $\delta \rightarrow 0$ limit, the exchange [01–12] of three consecutive particles is the dominant one.

An important observation that we should make at this point is that while the exponents themselves converge quite slowly to their $\delta \rightarrow 0$ values, the difference $\Delta\eta = \eta_{min} - \eta_\infty$ between the exponent obtained for infinite distance τ_0 between the instantons and that at the minimum converges much faster. Typically, one would have to go down to $\delta \sim 10^{-7}$ to obtain a value of the exponent that is in reasonable agreement with the result of the calculation using an unscreened Coulomb interaction. The calculation with $\delta \sim 10^{-4}$ gives an excellent approximation to the result for $\Delta\eta$ one would obtain with an unscreened Coulomb interaction. Use of the regularized Coulomb interaction simplifies the calculation significantly from two aspects: computational cost and complexity of the code involved.

Focusing on the three-particle exchange, we were able to extend the calculation to 25 spectators on each side of the exchanging triad, 50 spectators total. Figure 3 shows the evolution of $\Delta\eta$ as a function of the cutoff δ and the number of spectators that are allowed to move. We find that the value quickly saturates for decreasing δ . As mentioned above, the calculation with $\delta \sim 10^{-4}$ gives an excellent approximation to the result one would obtain with an unscreened Coulomb interaction.

With this extended data set, it is possible to extract the asymptotic behavior in the limit of large N . Neglecting logarithmic corrections, an excellent approximation

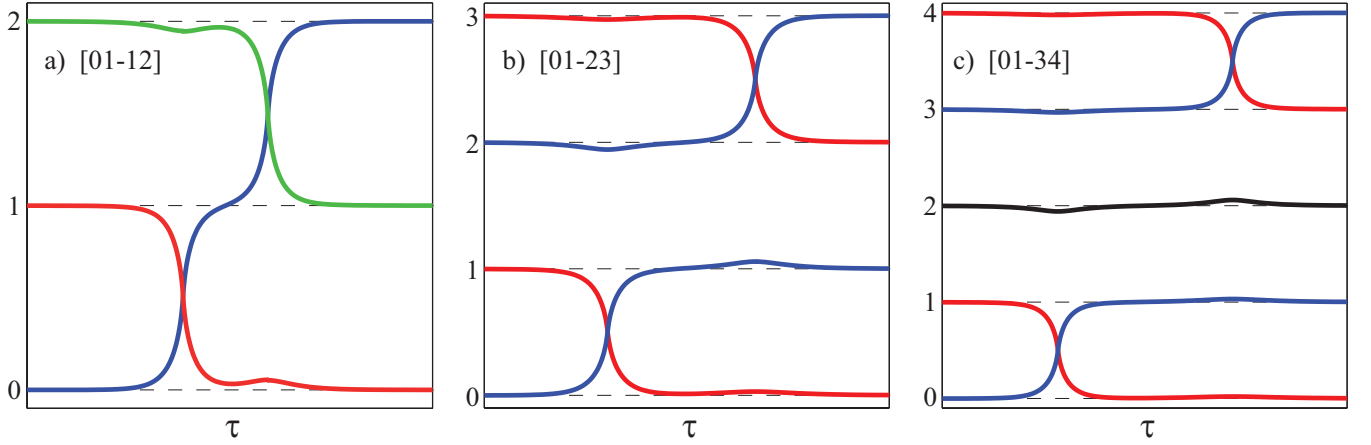


FIG. 1: (Panel a): The exchange of three particles as it unfolds in imaginary time. The numbers indicate the equilibrium positions of the exchanging particles. We call this type of exchange [01–12] following the convention introduced in the main text. The spectators, the other particles in the chain that extend indefinitely above and below, are assumed frozen in place and are not shown. (Panels b and c): The two most relevant exchanges in addition to [01–12]. We dub them [01–23] and [01–34], respectively, for obvious reasons. Note that in the case of [01–34], particle 2 is, in fact, a spectator.

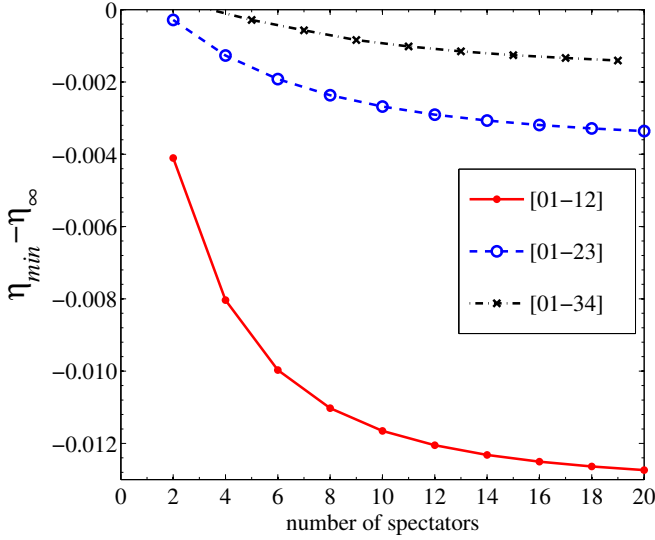


FIG. 2: A comparison of the difference $\Delta\eta = \eta_{min} - \eta_{\infty}$ between the exponent obtained for infinite distance τ_0 between the instantons and that at the minimum for the various kinds of exchanges considered here. [01–12], i.e. the three-particle exchange, dominates. The curves shown have been obtained using a cutoff $\delta = 10^{-3}$ for the Coulomb interaction, which is more than adequate for this kind of comparison. In fact, [01–23] and [01–34] have for all practical purposes converged to their $\delta \rightarrow 0$ values.

is the expression taken from Ref. [7]:

$$(\Delta\eta)_N = \Delta\eta + \frac{\alpha}{N^2}. \quad (27)$$

The above formula results in excellent fits, and we obtain $\Delta\eta_{0112} = -0.01324 \pm 0.00001$, and $\alpha_{0112} = 0.21 \pm 0.01$, in the limit where all particles participate in the three-particle exchange.

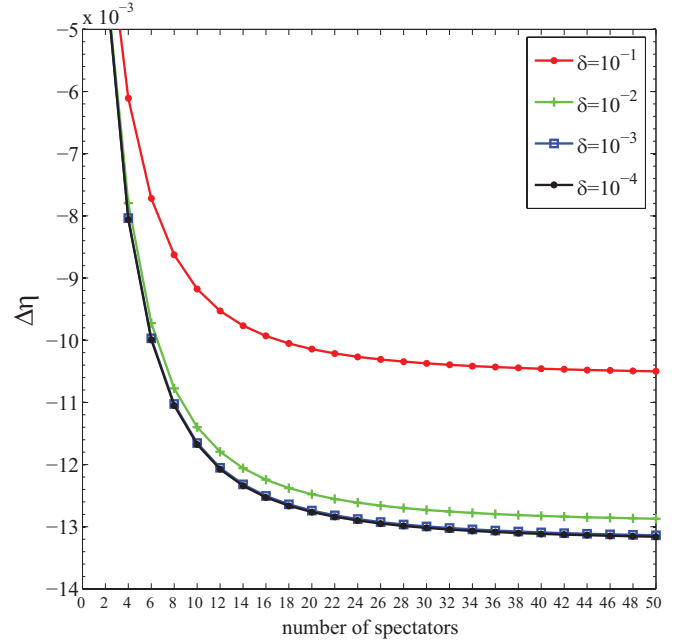


FIG. 3: The difference $\Delta\eta = \eta_{min} - \eta_{\infty}$ for the dominant three-particle exchange as a function of the cutoff δ used in the calculation. The result for $\delta = 10^{-4}$ is an excellent approximation to the result one would obtain with an unscreened Coulomb interaction.

Using a similar procedure and by comparing the value obtained from the extended data set and that shown in Fig. 2 we obtain estimates for the parameters relevant to the other two exchanges, [01–23] and [01–34]. In particular, we find that $\Delta\eta_{0123} = -0.0036 \pm 0.0002$, $\alpha_{0123} = 0.11 \pm 0.05$ and that $\Delta\eta_{0134} = -0.0016 \pm 0.0002$, $\alpha_{0134} = 0.08 \pm 0.05$.

B. Pre-exponential factor

As we saw in Sec. III A, the dimensionless instanton action $\tilde{\eta} < 2\eta$. This fact is important for the theory of equilibration of the Wigner crystal, see Sec. IV. In terms of the instanton trajectories, it is a consequence of the attraction of single instantons at large temporal distances. This attraction can be understood analytically, see Appendix B. On the other hand, the attraction is very weak, $\Delta\eta \sim 10^{-2}$. This implies that the three particle instanton consists of two single instantons, which are not significantly distorted by the interaction with each other, see Fig. 1(a). The approximation of two weakly coupled instantons enables us to find the pre-exponential factor \tilde{J}^* in the expression (25) for the exchange constant \tilde{J} while avoiding the evaluation of the fluctuation determinant near the instanton trajectory.

We start by considering the contribution of a single instanton to the path integral representing the evolution operator

$$I \int_0^{\mathcal{T}} dt = \frac{J}{2\hbar} \mathcal{T}. \quad (28)$$

Here I includes the instanton action and the integral over the Gaussian fluctuations near the instanton trajectory; the integral over the position of the instanton τ accounts for the zero mode. The right-hand side of Eq. (28) is obtained by isolating the contribution of the nearest neighbor exchange in the Hamiltonian (8) and expanding the evolution operator $e^{-H\mathcal{T}/\hbar}$ to first order in J . Equation (28) enables us to identify $I = J/2\hbar$.

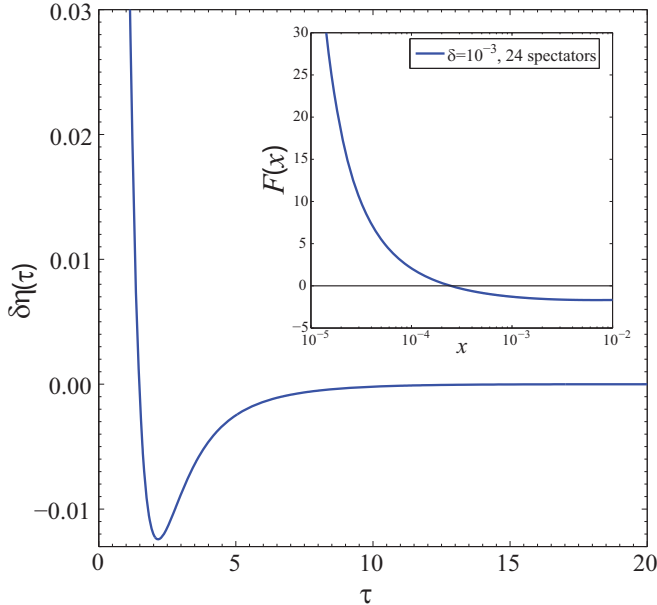


FIG. 4: Interaction between two instantons $\delta\eta(\tau) = \eta(\tau) - \eta_\infty$ at a temporal distance τ evaluated numerically. The inset shows the numerically evaluated function $F(x)$ defined by Eq. (31).

Next, we consider the contribution to the path integral due to a single three-particle exchange shown in Fig. 1(a)

$$I^2 \int_0^{\mathcal{T}} dt_1 \int_{\tau_1}^{\mathcal{T}} dt_2 e^{-\delta\eta(\tau_2-\tau_1)/\sqrt{na_B}} = \frac{\tilde{J}\mathcal{T}}{2\hbar} + \frac{1}{2} \left(\frac{J\mathcal{T}}{2\hbar} \right)^2. \quad (29)$$

Here the relation between $t_{1,2}$ and $\tau_{1,2}$ is given by Eq. (21). The quantity $\delta\eta(\tau)$ is defined as the difference between the action of a two-instanton trajectory with the distance τ between the instantons and the action $\eta_\infty = 2\eta$ of two instantons at infinite separation, $\tau \rightarrow \infty$; its minimum value coincides with $\Delta\eta$. The numerically evaluated $\delta\eta(\tau)$ is shown in Fig. 4. In the left-hand side of Eq. (29) we neglected the effect of the interaction between the instantons on the Gaussian fluctuations about the instanton trajectories. In the right-hand side we accounted for the fact that three-particle exchange processes appear as a result of the three-particle permutation operators (16) in the Hamiltonian, or in the second order perturbation theory in the nearest-neighbor exchange J . Using the relation $I = J/2\hbar$ we express \tilde{J} as

$$\tilde{J} = J^2 \frac{\varepsilon a_B}{2(na_B)^{3/2} e^2} F(na_B), \quad (30)$$

where

$$F(x) = \int_0^\infty \left[\exp\left(-\frac{\delta\eta(\tau)}{\sqrt{x}}\right) - 1 \right] d\tau. \quad (31)$$

The integral (31) converges because, as discussed in Appendix B, at large τ the interaction of single instantons falls off as $\delta\eta(\tau) \propto \tau^{-2}$, see Eq. (B10).

At $x \rightarrow 0$ the integral (31) can be evaluated in the saddle point approximation

$$F(x) = \sqrt{\frac{2\pi}{\delta\eta''}} x^{1/4} e^{-\Delta\eta/\sqrt{x}}, \quad (32)$$

where $\Delta\eta \approx -0.01324$ and $\delta\eta'' \approx 0.024$ are the values of $\delta\eta(\tau)$ and its second derivative at the minimum. Substituting Eq. (32) into (30) we find that \tilde{J} depends on na_B as

$$\tilde{J} \sim (na_B)^{5/4} \frac{e^2}{\varepsilon a_B} \exp\left(-\frac{2\eta + \Delta\eta}{\sqrt{na_B}}\right). \quad (33)$$

Note that the sign of the exchange constant is positive, and the pre-exponential factor up to a numerical factor coincides with the one for the nearest neighbor exchange (3). This is the expected behavior for any exchange process controlled by a well-defined instanton trajectory.

It is important to note that the saddle point approximation (32) holds only at $x \ll (\Delta\eta)^2$. In physical terms this means $na_B \ll 10^{-4}$. On the other hand, the WKB approximation is applicable under the less stringent condition $na_B \ll 1$. To evaluate the integral (31) in the intermediate region $10^{-4} \ll x \ll 1$ one can completely neglect the attraction of single instantons and the shallow minimum of $\delta\eta(\tau)$ associated with it. Instead, one should

notice the strong repulsion of the cores of the instantons at short distances. Taking this repulsion into consideration, one can approximate the integrand of Eq. (31) by $-\theta(\tau_0 - \tau)$, where $\theta(x)$ is the unit step function, and $\tau_0(x)$ is defined as the solution of the equation $\delta\eta(\tau_0) = x^{1/2}$. This yields

$$F(x) = -\tau_0(x). \quad (34)$$

The cores of single instantons repel exponentially, $\delta\eta(\tau) \sim e^{-\lambda\tau}$ with $\lambda \sim 1$. In that case $\tau_0(x)$ depends on x logarithmically, and we find

$$F(x) = -\frac{1}{2\lambda} \ln \frac{1}{x}. \quad (35)$$

Interestingly, the results (34) and (35) are negative. This means that the next nearest neighbor exchange constant (30) has ferromagnetic sign only at $na_B < x^*$, where $x^* \sim 10^{-4}$, and becomes antiferromagnetic at higher densities, $na_B > x^*$. In this regime

$$\tilde{J} \sim -J^2 \frac{\varepsilon a_B}{(na_B)^{3/2} e^2} \ln \frac{1}{na_B}. \quad (36)$$

The result of numerical evaluation of $F(x)$ is shown in Fig. 4. The sign of the exchange constant (30) changes at $na_B = x^* \approx 3 \times 10^{-4}$.

IV. RATE OF FULL EQUILIBRATION OF THE WIGNER CRYSTAL AT LOW TEMPERATURES

In Secs. II and III we studied the corrections to the leading-order Hamiltonian of the Wigner crystal given by Eqs. (1) and (2). These corrections break the integrability of the problem and give rise to the scattering of excitations. As a result, the system relaxes to thermodynamic equilibrium. In this section we study the corresponding equilibration rate in the regime of low temperatures, $T \ll J$.

This problem has been solved previously for weakly interacting electrons,¹⁰ for the spinless Wigner crystal,¹⁷ as well as for a spinless quantum liquid with arbitrary interaction strength.^{18,19,23} The equilibration proceeds in two stages. First, the low-energy excitations collide with each other and achieve thermal equilibrium. At low temperatures the momenta of these excitations are small, $p \ll \hbar n$, and to a first approximation the collisions conserve the total momentum of the excitations P_{ex} . As a result, the equilibrium state of the gas of excitations is characterized by $P_{\text{ex}} \neq 0$. This first stage of the equilibration process proceeds relatively quickly, with the typical relaxation time τ_0 following a power-law temperature dependence.

The second stage of the equilibration process involves slow relaxation of P_{ex} to its equilibrium value. For a system at rest, the total momentum of the excitations in equilibrium is zero, and the approach to equilibrium follows the usual relaxation law

$$\dot{P}_{\text{ex}} = -\frac{P_{\text{ex}}}{\tau}. \quad (37)$$

The microscopic processes driving the relaxation (37) involve excitations diffusing in momentum space from the vicinity of one Fermi point to the other. The bottleneck in this process is the center of the Fermi sea where the excitation energy reaches its maximum value Δ . As a result, the rate of full equilibration follows the activated temperature dependence $\tau^{-1} \propto e^{-\Delta/T}$.

In a spinless system, the excitation with the lowest energy in the center of the Fermi sea is essentially a hole dressed by electron-electron interactions. The full expression for the equilibration rate is given by¹⁸

$$\tau^{-1} = \frac{3\hbar k_F^2 B}{\pi^2 \sqrt{2\pi m^* T}} \left(\frac{\hbar v}{T} \right)^3 e^{-\Delta/T}. \quad (38)$$

Here, k_F is the Fermi wave vector and v is the velocity of the low-energy excitations. The parameters m^* and B are, respectively, the effective mass and the diffusion constant in momentum space for the hole excitation at the center of the Fermi sea. The temperature dependence of the diffusion constant is given by

$$B = \frac{4\pi^3 n^2 T^5}{15\hbar^5 m^2 v^8} \left(\Delta'' - \frac{2v'}{v} \Delta' + \frac{\Delta'^2}{m^* v^2} \right)^2. \quad (39)$$

The primes in Eq. (39) denote derivatives with respect to the particle density n . We shall now discuss how these results change in the presence of spins.

A. Equilibration rate for a Wigner crystal at $T \ll J$

The general picture of two-stage relaxation also applies to systems with spins. In this case there are two types of low-energy excitations in the system, corresponding to the charge and spin degrees of freedom. For instance, at strong interactions the charge excitations are the phonons in the Wigner crystal, cf. Eq. (13), whereas the elementary excitations of the spin Hamiltonian (2) are the so-called spinons with the excitation spectrum^{24,25}

$$\epsilon(q) = \frac{\pi J}{2} \sin q. \quad (40)$$

Here the wavevector of the excitations on the spin chain is related to their physical momentum as $q = p/\hbar n$.

Because of the smallness of the exchange constant J in Eq. (40), the spinons are the lowest-energy excitations of the system at any given momentum, see Fig. 5. Thus the full equilibration of the Wigner crystal is achieved by their diffusion in momentum space, similar to that of the holes in spinless systems. We therefore conclude that the activation energy Δ that will appear in the generalization of Eq. (38) to the spin-degenerate case will be given by the maximum energy of the spinon, and the effective mass will be determined by the curvature of $\epsilon(q)$ near the maximum,

$$\Delta = \frac{\pi J}{2}, \quad \frac{1}{m^*} = \frac{\pi J}{2\hbar^2 n^2}. \quad (41)$$

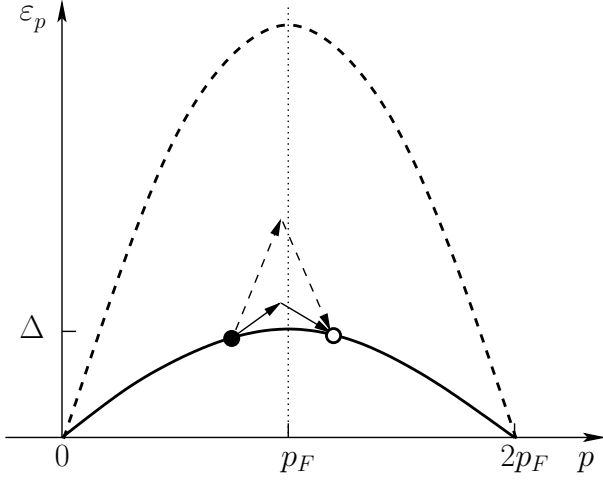


FIG. 5: The spectrum of elementary excitations of a one-dimensional Wigner crystal consists of two branches, phonons and spinons, shown by dashed and solid lines, respectively. Equilibration of the system is controlled by the scattering processes in which a quasiparticle crosses the edge of the Brillouin zone $p = p_F$, i.e., umklapp processes. At low temperatures the occupation numbers of the excitations at the edge of the Brillouin zone are exponentially small. Because the energy of a spinon with momentum p_F is much smaller than that of a phonon, the contribution of the latter is negligible. Each umklapp process includes absorption of one acoustic excitation and emission of another one. Processes involving two acoustic phonons and two acoustic spin excitations are shown by thin dashed and solid lines, respectively. Mixed processes involving one of each type of acoustic excitations are also allowed.

At q near 0 or π the spinon spectrum is linear with the velocity

$$v_\sigma = \frac{\pi J}{2\hbar n}. \quad (42)$$

Such low-energy spin excitations can be equivalently represented in terms of the bosons in the Tomonaga-Luttinger liquid, which for particles with spin is described by the Hamiltonian¹

$$H_{\text{TL}} = \sum_p [v_\rho |p| b_p^\dagger b_p + v_\sigma |p| c_p^\dagger c_p]. \quad (43)$$

Here b_p and c_p are the bosonic annihilation operators of the charge and spin excitations, while v_ρ and v_σ are the corresponding velocities.

At the first stage of the equilibration process the bosonic excitations collide with each other, and their distribution function relaxes to the equilibrium form

$$N_p^{(\rho,\sigma)} = \frac{1}{e^{(v_{\rho,\sigma}|p|-up)/T} - 1}. \quad (44)$$

These equilibration processes are caused by the integrability-breaking perturbations (15), (17), and (19). Because typical excitations participating in this process

have energies of order temperature, the relaxation rate τ_0^{-1} is only power-law small in T . Compared with the exponentially slow rate of full relaxation (38), these processes can be considered instantaneous, and the magnitude of τ_0^{-1} has no effect on the subsequent discussion.

The parameter u in Eq. (44) accounts for momentum conservation in the boson collisions. The total momentum of the gas of excitations is then easily found,

$$P_{\text{ex}} = \frac{\pi L T^2}{3\hbar} \left(\frac{1}{v_\rho^3} + \frac{1}{v_\sigma^3} \right) u. \quad (45)$$

It is important to keep in mind that Eq. (45) is not the full momentum of the system. In the Luttinger liquid theory the latter is given by²⁶

$$P = p_F(N^R - N^L) + P_{\text{ex}}, \quad (46)$$

where the zero modes N^R and N^L have the meanings of the total numbers of the right- and left-moving electrons in the system. The first term in Eq. (46) accounts for the simple fact that even in the absence of excitations the system can move as a whole and thus have a nonvanishing momentum.

At $u > 0$ the occupation numbers of the bosonic acoustic excitations (43) depend on the direction of motion, with the right-moving states being more populated than the left-moving ones at the same energy. Thus when spinons with momenta near p_F collide with acoustic excitations, their momentum is more likely to increase than decrease. This gives rise to a net current of spinons in momentum space through the edge of the Brillouin zone $p = p_F$, see Fig. 5. As a result of such umklapp scattering processes the right-moving spinons convert to left-moving ones, leading to a decrease of velocity u . Since the total momentum (46) of the system is conserved, during this second stage of the equilibration process the momentum is being transferred from excitations to the zero modes.^{13,23} This corresponds to backscattering of electrons in the system. The resulting effects on the electronic transport are discussed in Sec. V.

At low temperature $T \ll \Delta$ the typical change of momentum $T/v_{\rho,\sigma}$ in the processes shown in Fig. 5 is small compared to the typical scale $\sqrt{m^*T}$ at which the spinon distribution function varies near the edge of the Brillouin zone. This enables one to evaluate the rate of change of the momentum of excitations \dot{P}_{ex} using the Fokker-Planck equation for the spinon distribution function

$$\partial_t f = -\partial_p J, \quad J = -\frac{B}{2} \left[\frac{\varepsilon'_p}{T} + \partial_p \right] f, \quad (47)$$

where $\varepsilon_p = \epsilon(p/\hbar n)$. By imposing the boundary conditions on the distribution function obtained with the help of Eq. (44), one finds

$$\dot{P}_{\text{ex}} = -u \frac{2L\hbar^3 k_F^2 B}{\pi T \sqrt{2\pi m^* T}} e^{-\Delta/T}. \quad (48)$$

The derivation is identical to the case of diffusion of holes in a spinless system,^{17,18,23} with the exception of a factor of 2 accounting for two possible spin polarizations of spinons. In this approach the diffusion constant B appears as a phenomenological parameter. Its evaluation requires a microscopic treatment of the coupling of the spinons to the bosonic excitations, and will be discussed below.

We can now combine the results (45) and (48) with the definition (37) of the equilibration time τ . The resulting expression coincides with Eq. (38) with the substitution $v^3 \rightarrow 2/(v_\rho^{-3} + v_\sigma^{-3})$. Taking advantage of the fact that in the Wigner crystal $v_\sigma \ll v_\rho$ and using Eqs. (41) and (42), the result can be brought to the form

$$\tau^{-1} = \frac{3\pi^3 B}{32n^2} \left(\frac{J}{T}\right)^{7/2} \exp\left(-\frac{\pi J}{2T}\right). \quad (49)$$

In a system described by the leading-order Hamiltonian (1), (2) integrability results in a vanishing diffusion constant B . To evaluate it, one has to consider the corrections to the Hamiltonian discussed in Sec. II.

B. Diffusion of spinons in momentum space

The parameter B in the expression (49) for the equilibration rate has the meaning of the diffusion constant describing the motion of spinons in momentum space near the top of the spinon spectrum. It is formally defined¹⁸ as

$$B = \frac{1}{\hbar^2} \sum_{\delta p} (\delta p)^2 W(\delta p), \quad (50)$$

where $W(\delta p)$ is the rate of the scattering events changing the spinon momentum by δp . The scattering originates from the interaction of the spinon with the low-energy excitations of the system described by Eq. (43).

It is convenient to classify the low-energy excitations as belonging to one of the four branches, ρR , ρL , σR , and σL , depending on their charge or spin nature, and the direction of motion. Because the velocity of the spinon near the top of the spectrum is small compared to both v_σ and v_ρ , scattering processes involving excitations in only one of the four branches are forbidden by conservation of momentum and energy. Thus, the dominant scattering processes involve two branches, and the scattering rate has the following general form

$$W(\delta p) = \frac{1}{2} \sum_{\alpha, \beta} \sum_{a, e} W_{ae}^{\alpha\beta}(\delta p). \quad (51)$$

Here a and e label the branches from which excitations are absorbed and emitted, respectively, whereas α and β denote the spin projections of the spinon before and after the scattering event. The partial scattering rates

are obtained from Fermi's golden rule,

$$W_{ae}^{\alpha\beta}(\delta p) = \frac{2\pi}{\hbar} \sum_{p_a, p_e} M_{p_a p_e}^{\alpha\beta}(\delta p) \delta(\epsilon_p - \epsilon_{p+\delta p} + v_a p_a - v_e p_e). \quad (52)$$

Here v_a and v_e denote the velocities of the absorption and emission branches, which according to Eq. (43) are $v_{\rho R} = -v_{\rho L} = v_\rho$ and $v_{\sigma R} = -v_{\sigma L} = v_\sigma$. Momentum conservation is ensured by the matrix element of the T -matrix entering the definition

$$M_{p_a p_e}^{\alpha\beta}(\delta p) = \sum_{i, f} w_i |\langle f; \beta, p + \delta p | \hat{T} | i; \alpha, p \rangle|^2 \times \delta_{P_a^f, P_a^i - p_a} \delta_{P_e^f, P_e^i + p_e}. \quad (53)$$

In this expression i and f refer to the initial and final states of the Luttinger liquid, w_i is the Gibbs weight of the initial state, p and $p + \delta p$ are the values of the spinon momentum before and after the collision. Finally, $P_a^{i(f)}$ is the total initial (final) momentum of the excitation branch a , and $P_e^{i(f)}$ is that for branch e .

Each of the indices a and e in Eq. (51) takes one of the four values, ρR , ρL , σR , and σL , resulting in 16 possible contributions to the scattering rate. It is convenient to group these contributions into three classes, determined by the charge or spin nature of the two branches participating in spinon scattering. Accordingly, the diffusion constant (50) is presented as a sum of three contributions

$$B = B_{\rho\rho} + B_{\rho\sigma} + B_{\sigma\sigma}. \quad (54)$$

Here $B_{\rho\rho}$ accounts for the four types of processes in which a and e are chosen from the branches ρR and ρL , the contribution $B_{\sigma\sigma}$ accounts for the four terms in which only σR and σL branches are involved, and $B_{\rho\sigma}$ includes the eight remaining types of processes. To evaluate the three contributions to B we need to consider the coupling of the spinon to the acoustic spin and charge excitations.

1. Effective Hamiltonian of the spinon interacting with acoustic excitations

The general form of the Hamiltonian of the Wigner crystal discussed Sec. II is valid in a rather wide temperature interval $T \ll (e^2/\epsilon a_B)(na_B)^{7/4}$. In order to discuss equilibration of the system at $T \ll J$ where the density of high-energy spinons is exponentially small it is sufficient to consider the interaction of a single spinon with acoustic spin and charge excitations. To this end we introduce an effective Hamiltonian describing the motion of a spinon coupled to the acoustic modes.

In the low-energy limit the acoustic modes are described by the Tomonaga-Luttinger Hamiltonian (43). In the effective theory, the spinon is treated as a mobile impurity with spectrum (40) and spin \mathbf{S} . The Hamiltonian of a free spinon can be written as

$$H_{\text{sp}}^{(0)} = \epsilon(-ia\partial_Y) \simeq \Delta - \frac{\hbar^2(-i\partial_Y - \pi n/2)^2}{2m^*}. \quad (55)$$

The last expression in Eq. (55) is valid near the top of the spinon spectrum, and the values of Δ and m^* are given by Eq. (41).

The parameter $\Delta = \pi J/2$ in Eq. (55) depends on the particle density n . This enables us to obtain the coupling of the spinon to the phonons following the procedure of Sec. IID,

$$\hat{V}_{\text{ph}} = -nu'(Y)\Delta', \quad (56)$$

where $\Delta' = d\Delta/dn$, cf. Eq. (39).

Quite generally, the coupling of an impurity with spin \mathbf{S} to the low-energy spin degrees of freedom may be described by a perturbation of the form

$$\hat{V}_K = J_K^R \mathbf{S} \cdot \mathbf{s}^R(Y) + J_K^L \mathbf{S} \cdot \mathbf{s}^L(Y).$$

Here Y is the position of the spinon in Lagrangian variables defined as $y = la$.¹⁹ A Hamiltonian of this form was applied recently to the related problem of a mobile impurity with spin in a one-dimensional Fermi gas.²⁷ The spin densities $\mathbf{s}^R(Y)$ and $\mathbf{s}^L(Y)$ associated with the right- and left-moving excitations at the position Y of the impurity are easily expressed in terms of the creation and annihilation operators of the one-dimensional fermions considered in Ref. 27. Upon bosonization, the expressions for the z components take the forms

$$s_z^{R,L}(Y) = \mp \frac{i}{2} \sum_p \sqrt{\frac{|p|}{\pi\hbar L}} \theta(\pm p) (c_p e^{ipY/\hbar} - c_p^\dagger e^{-ipY/\hbar}). \quad (57)$$

By virtue of the universality of the Luttinger liquid theory, this expression applies at any strength of interaction between electrons. The expressions for the x and y components of the spin densities are more complicated, but their explicit forms will not be used in this paper. For the spinon near the top of the spectrum, the constants J_K^R and J_K^L are equal to each other and will be denoted by J_K . Thus, the operator \hat{V}_K takes the form

$$\hat{V}_K = J_K \mathbf{S} \cdot [\mathbf{s}^R(Y) + \mathbf{s}^L(Y)]. \quad (58)$$

The operators (56) and (58) describe the coupling of the spinon to a single bosonic excitation. In principle, the spinon can interact with an arbitrary number of bosons. Of all such perturbations we will only need the explicit form of the operator that couples the spinon to one charge- and one spin-excitation. It can be obtained by noticing that the coupling constant J_K in Eq. (58) depends on density and applying the procedure of Sec. IID,

$$\hat{V}_2 = -nu'(Y)J_K' \mathbf{S} \cdot [\mathbf{s}^R(Y) + \mathbf{s}^L(Y)]. \quad (59)$$

Finally, the evaluation of the diffusion constant B requires consideration of the coupling of the acoustic spin and charge modes to each other. We start by rewriting the spin part of the Hamiltonian (43) in terms of the z -components of spin density operators (57) as

$$\sum_p v_\sigma |p| c_p^\dagger c_p = 2\pi\hbar \int v_\sigma \left\{ [s_z^L(y)]^2 + [s_z^R(y)]^2 \right\} dy. \quad (60)$$

Noticing that v_σ depends on the electron density and applying the procedure of Sec. IID again we obtain the perturbation of the form

$$\hat{V}_{\rho\sigma} = -2\pi\hbar n v_\sigma' \int u'(y) \left\{ [s_z^L(y)]^2 + [s_z^R(y)]^2 \right\} dy. \quad (61)$$

It is important to note that the operator (61) couples a phonon to two spin excitations moving in the same direction. The Hamiltonian also contains the perturbation that couples a single phonon to one right-moving and one left-moving spin boson. To obtain its explicit form we need to consider the correction¹ to the spin sector of the Tomonaga-Luttinger Hamiltonian (60),

$$H_g = -2\pi\hbar g v_\sigma \int \mathbf{s}^R(y) \cdot \mathbf{s}^L(y) dy. \quad (62)$$

At low energies this perturbation scales to zero logarithmically, $g = 1/\ln(J/T)$. The density dependence of v_σ yields a coupling of the form

$$\hat{V}_g = 2\pi\hbar g n v_\sigma' \int u'(y) \mathbf{s}^R(y) \cdot \mathbf{s}^L(y) dy. \quad (63)$$

To summarize, in the effective low-energy theory the spinon is a mobile impurity in the Tomonaga-Luttinger liquid (43). It is described by the free-spinon Hamiltonian (55), and the various perturbations (56), (58), (59), (61), and (63).

The perturbations (56) and (58) are nominally marginal, and the remaining ones are irrelevant. The perturbation (56) does not scale at all, whereas (58) scales logarithmically at low energies. The scaling of the coupling constant J_K can be understood by noticing that the perturbation of the form (58) describes the two-channel Kondo problem.²⁷

Positive J_K corresponds to the antiferromagnetic Kondo problem. In that case, the coupling constant grows at low energies, and the two-channel Kondo problem scales to an intermediate-coupling fixed point,²⁸ where the impurity spin is fully screened. The enhanced coupling suppresses the mobility of the impurity²⁷ to $\mu \propto T^{-2}$, compared to $\mu \propto T^{-4}$ in the spinless case.²⁹ As a result, the diffusion constant in momentum space, $B = 2T/\mu$,³⁰ should scale as $B \propto T^3$, in contrast to $B \propto T^5$ for a spinless impurity.¹⁸

Our interest in diffusion of mobile impurities is motivated by the problem of scattering of spinon excitations in the Heisenberg chain (2). Their spins are not screened even at $T = 0$, indicating that the coupling constant J_K may not be positive. Negative J_K corresponds to the ferromagnetic Kondo problem, in which the coupling constant scales to zero logarithmically, and the impurity spin remains unscreened. This form of scaling of the coupling of spinons to low-energy spin excitations in one-dimensional Fermi systems was discussed in Ref. 31. At finite temperatures the scaling suppresses the coupling constants by a factor of order $\ln(J/T)$, which will not play an important role in our theory compared to the

much stronger temperature dependence of the equilibration rate (49).

2. Scattering of spinons by charge excitations

We start the evaluation of the diffusion constant B by studying the contribution $B_{\rho\rho}$ originating from the coupling of the spinon to the charge excitations of the Wigner crystal. The latter are phonons discussed in Sec. II B. The spinon couples to phonons because its energy $\epsilon \sim J$ depends on the electron density. It is important to note that such a coupling is insensitive to the spin degree of freedom of the spinon. In that sense, the problem is equivalent to that of a spinless mobile impurity diffusing in a Luttinger liquid.²⁹ The diffusion constant in momentum space was expressed¹⁸ in terms of the spectrum of the impurity and its dependence on density, and is given by Eq. (39). We thus obtain $B_{\rho\rho}$ by substituting $\Delta = \pi J/2$ and $v = v_\rho$ into the above expressions. Because of the exponential dependence (3) of J on density, the first term in the parentheses in Eq. (39) gives the dominant contribution, and we find

$$B_{\rho\rho} = \frac{\pi^5 \eta^4}{240} \frac{T^5 J^2}{\hbar^5 n^4 a_B^2 m^2 v_\rho^8}. \quad (64)$$

The phonon velocity v_ρ can be obtained from Eq. (12). At $q \rightarrow 0$ one finds

$$v_\rho = \frac{\sqrt{2\mathcal{L}}}{\hbar n} \frac{e^2}{\varepsilon a_B} (na_B)^{3/2}. \quad (65)$$

Theoretically, the parameter \mathcal{L} diverges logarithmically at $q \rightarrow 0$, see Appendix A. On the other hand, the scattering of the spinons is dominated by thermal phonons, for which

$$\mathcal{L} = \ln \frac{e^2 (na_B)^{3/2}}{\varepsilon a_B T}. \quad (66)$$

Alternatively, if the Coulomb interaction is screened by a metal gate at a distance d from the Wigner crystal, the divergence is cut off as $\mathcal{L} = \ln(nd)$.

3. Mixed scattering processes

We now consider the contribution $B_{\rho\sigma}$ to the diffusion constant (54). This contribution accounts for the scattering processes in which one of the two branches a and e belongs to the charge sector and the other to the spin sector. The first step is to obtain the corresponding term in the T -matrix using the standard perturbative expression

$$\hat{T} = \hat{V} + \hat{V} \frac{1}{E_i - H_0} \hat{V} + \dots, \quad (67)$$

where E_i is the energy of the initial state. We are interested in the on-shell matrix elements for which the

energies in the initial and final states are equal. The relevant contribution has the form

$$t_m n u'(Y) \mathbf{S} \cdot [\mathbf{s}^R(Y) + \mathbf{s}^L(Y)]. \quad (68)$$

Similar to Eq. (39), there are three contributions to t_m arising from different perturbations in the effective Hamiltonian.

The simplest contribution is obtained by applying the perturbation (59) in the first order,

$$t_m^{(1)} = -J'_K. \quad (69)$$

This contribution is analogous to the first term in Eq. (39). The other two contributions arise in the second order perturbation theory. Combining the perturbations \hat{V}_K and $\hat{V}_{\rho\sigma}$ given by Eqs. (58) and (61) in the second order we obtain

$$t_m^{(2)} = J_K \frac{v'_\sigma}{v_\sigma}. \quad (70)$$

This contribution is analogous to the second term in Eq. (39). In this process \hat{V}_K describes scattering of a spinon off of a virtual spin boson, and $\hat{V}_{\rho\sigma}$ describes the interaction of the latter with the charge and spin bosons present in the initial and final states. The final contribution arises in second order in the perturbations \hat{V}_{ph} and \hat{V}_K given by Eqs. (56) and (58). It describes the scattering process in which the spinon interacts sequentially with the spin and charge bosons present in the initial and final states. In this process, the absorption of the initial state boson and the emission of the final state boson can happen in a different order, which leads to a near cancellation of the corresponding contributions. A finite result arises only due to the curvature of the spinon spectrum and is given by

$$t_m^{(3)} = \text{sgn}(p_a p_e) \frac{\Delta' J_K}{m^* v_\rho v_\sigma}, \quad (71)$$

where m^* is defined in Eq. (41). This contribution is analogous to the last term in Eq. (39).

The full matrix element t_m in Eq. (68) is given by the sum of the contributions (69)–(71). At low densities all three contributions are exponentially small. For the Heisenberg model (2) the quantities J_K and v_σ are controlled by a single parameter J . As a result the combined contribution

$$t_m^{(1)} + t_m^{(2)} = J_K \left[\frac{v'_\sigma}{v_\sigma} - \frac{J'_K}{J_K} \right] \quad (72)$$

vanishes. A nonvanishing result appears only if one takes into account next nearest neighbor exchange coupling \tilde{J} . Using Eq. (33) we conclude

$$t_m^{(1)} + t_m^{(2)} \propto \tilde{J} \propto \exp\left(-\frac{2\eta + \Delta\eta}{\sqrt{na_B}}\right). \quad (73)$$

Noticing that $\Delta \sim nJ_k \sim J$ and that $m^*v_\sigma = \hbar n$ we find

$$t_m^{(3)} \propto J^2 \propto \exp\left(-\frac{2\eta}{\sqrt{na_B}}\right). \quad (74)$$

Keeping in mind that $\Delta\eta \approx -0.013$, we conclude that in the limit of low density Eq. (73) gives the dominant contribution to t_m , but at $na_B < 10^4$ the difference between the exponents in Eqs. (73) and (74) is insignificant.

In order to obtain the contribution $B_{\rho\sigma}$ to the diffusion constant (54) we substitute Eq. (68) into Eq. (53) and obtain

$$M_{p_a p_e}^{\alpha\beta}(\delta p) = t_m^2 (\delta_{\alpha,\beta} + 2\delta_{\alpha,-\beta}) \delta_{p_a - p_e, \delta p} \\ \times \frac{n|p_a p_e|}{8\pi\hbar m v_\rho L^2} N_{p_a}^{(a)} (N_{p_e}^{(e)} + 1), \quad (75)$$

where $N_p^{(a,e)}$ denote either $N_p^{(\rho)}$ or $N_p^{(\sigma)}$, depending on the nature of the a and e branches, and are given by Eq. (44) with $u = 0$. Then, using Eqs. (50)–(52), we find

$$B_{\rho\sigma} = t_m^2 \frac{2\pi^2 n T^5}{5\hbar^6 m v_\rho^3 v_\sigma^4}. \quad (76)$$

In analogy with the result (64) for $B_{\rho\rho}$, the contribution (76) scales as T^5 . On the other hand, the exponentially small velocity of the spin excitations v_σ in the denominator of Eq. (76) enhances $B_{\rho\sigma}$ as compared to $B_{\rho\rho}$,

$$\frac{B_{\rho\rho}}{B_{\rho\sigma}} \propto \exp\left(-\frac{2\eta}{\sqrt{na_B}}\right), \quad (77)$$

where we used the estimate (74) for t_m . From Eq. (77) we conclude that at low electron density $B_{\rho\sigma} \gg B_{\rho\rho}$.

4. Scattering of spinons by spin excitations

We now turn to the contribution $B_{\sigma\sigma}$ to the diffusion constant (54). It arises from the scattering processes in which both the a and e branches belong to the spin sector. The leading contribution to the T -matrix appears in the second order with perturbations (58) and (62). For a spinon near the top of the spectrum the on-shell part is given by

$$-\frac{i}{L} J_K (J_K + 2\pi\hbar g v_\sigma) \sum_p \frac{e^{2ipY/\hbar}}{v_\sigma p} \mathbf{S} \cdot [\mathbf{s}^R(p) \times \mathbf{s}^L(p)], \quad (78)$$

where we have introduced the Fourier transforms of the spin density operators via

$$\mathbf{s}^{R,L}(Y) = \frac{1}{\sqrt{L}} \sum_p \mathbf{s}^{R,L}(p) e^{ipY/\hbar}. \quad (79)$$

It is important to note that the scattering matrix elements are enhanced at small momenta p by the denominator in Eq. (78). Similar contributions proportional to

$1/p$ in the second-order calculations for the $\rho\rho$ and $\rho\sigma$ channels cancel each other. The absence of such a cancellation in the $\sigma\sigma$ channel is due to the noncommutativity of the spin operators in the perturbations (58) and (62). The enhancement of quasiparticle scattering in the presence of spins was first pointed out in Ref. 32. It is worth noting that the nonlocal nature of Eq. (78) precludes the possibility of such terms appearing as perturbations in the Hamiltonian of a spinon interacting with the Tomonaga-Luttinger liquid. We therefore do not expect first order contributions to the T -matrix of the form (78).

Combining Eqs. (78) and (50)–(53), we obtain the contribution to the diffusion constant in the form

$$B_{\sigma\sigma} = \frac{J_K^2 (J_K + 2\pi\hbar g v_\sigma)^2 T^3}{8\pi\hbar^7 v_\sigma^6}. \quad (80)$$

The aforementioned enhancement of the scattering in the spin-spin channel results in $B_{\sigma\sigma} \propto T^3$, compared to the T^5 dependence of $B_{\rho\rho}$ and $B_{\rho\sigma}$. An analogous dependence $B \propto T^3$ was recently predicted in the limit of weakly interacting electrons.³³

At strong interactions, the magnitude of $B_{\sigma\sigma}$ is controlled by the coupling constants J_K and v_σ . In a Heisenberg chain (2) there is only a single energy scale, J . Thus, one expects $J_K \sim -gJ/n$, where the logarithmic factor $g = 1/\ln(J/T)$ appears as a result of the usual renormalization of the ferromagnetic Kondo coupling constant. Taking into account the expression (42) for v_σ , we conclude that the two terms in the combination $J_K + 2\pi\hbar g v_\sigma$ in Eq. (80) are of the same order of magnitude, and of opposite signs. On the other hand, the integrability of the Heisenberg model precludes real scattering processes, i.e., the above combination of the coupling constants must vanish.

Nonvanishing scattering appears due to perturbations that break the integrability of the spin chain (2). The simplest such perturbation is the next-nearest neighbor coupling \tilde{J} . Its presence results in $J_K + 2\pi\hbar g v_\sigma \propto \tilde{J}/n$. Substituting this estimate into Eq. (80) and omitting the logarithmic factors, we obtain

$$B_{\sigma\sigma} \sim \frac{n^2}{\hbar} \frac{\tilde{J}^2 T^3}{J^4}. \quad (81)$$

This estimate applies at $T \lesssim J$. Comparing Eq. (81) with the estimate of $B_{\rho\sigma}$ given by Eqs. (73) and (76) we find

$$\frac{B_{\rho\sigma}}{B_{\sigma\sigma}} \propto \exp\left(-\frac{2\eta}{\sqrt{na_B}}\right) \quad (82)$$

at $T \sim J$; the ratio is even lower at $T \ll J$.

In addition to the next-nearest neighbor coupling in the spin chain, the integrability of the problem is also broken by the spin-charge coupling. The leading contribution to $B_{\sigma\sigma}$ in this mechanism is obtained in second order in perturbations (56) and (63), whereby a spinon is coupled to acoustic spin excitations via an exchange

of a virtual phonon. Instead of \tilde{J} , such contributions to $B_{\sigma\sigma}$ contain J^2 , and result in essentially the same estimate (82). [See an analogous discussion below Eq. (74).] However, the processes of coupling by a virtual phonon do not involve noncommuting spin operators, and thus lack the enhancement of the scattering due to the small momentum in the denominator of Eq. (78). As a result, their contributions to $B_{\sigma\sigma}$ scale as T^5 , and are small compared to Eq. (80) at $T \ll J$. We therefore conclude that among the three terms in the diffusion coefficient (54), the spin channel contribution (80) always dominates.

V. SUMMARY AND DISCUSSION

The results obtained in this paper enable us to obtain the temperature dependent correction to the conductance of quantum wires at strong interactions in the spin-degenerate case. Previously such corrections at strong interactions were studied only for spin-polarized electrons.^{13,17} The spin-degenerate case represents a significantly more complicated problem, whose treatment requires consideration of all perturbations breaking integrability of the model, carried out above. We start by summarizing our results.

In Sec. II we identified three types of perturbations to the Hamiltonian (1), (2) of the one-dimensional Wigner crystal. They include the anharmonic corrections (15) in the charge sector, the next-nearest neighbor exchange of the spins (17), and the coupling of the charge and spin degrees of freedom (19). The magnitude of the next-nearest neighbor exchange was obtained by numerical treatment of the WKB action in Sec. III.

All of the above perturbations break integrability of the Hamiltonian (1), (2), and thus enable scattering of quasiparticle excitations off each other. In Sec. IV we applied these results to the evaluation of the rate of full equilibration of the one-dimensional Wigner crystal. We have found that the dominant process of equilibration involves scattering of a high-energy spinon by two acoustic spin excitations. The resulting equilibration rate is given by Eq. (49), with the dominant contribution to the spinon diffusion constant B given by Eq. (80). Using Eq. (81) one estimates the equilibration rate as

$$\tau^{-1} \sim \frac{\tilde{J}^2}{\hbar\sqrt{JT}} \exp\left(-\frac{\pi J}{2T}\right). \quad (83)$$

The magnitude \tilde{J} of the next-nearest neighbor coupling is given by Eq. (30).

As one can see from Eq. (46), conservation of the total momentum of the electron liquid means that the full equilibration is accompanied by backscattering of electrons. This enables one to relate the equilibration rate to the conductance of long uniform quantum wires.^{10,13} For example, in the limit of strong interactions, the interaction induced correction to the quantum conductance $2e^2/h$ is

given by

$$\delta G = -\frac{2e^2}{h} \frac{8\hbar n T^2}{3\pi^3 J^3} \frac{L}{\tau}. \quad (84)$$

The correction grows with the length of the wire L and eventually saturates at $L \sim J\tau/\hbar n$.¹³ In the shorter wires the correction to the quantized conductance is proportional to the equilibration rate τ^{-1} . Combining Eqs. (83) and (84) one then obtains $\delta G \propto T^{3/2} \exp(-\pi J/2T)$. The activated behavior of the correction to conductance of quantum point contacts was observed experimentally.³⁴ The activation temperature reported in Ref. 34 was rather small, $T_A \sim 1\text{K}$, and grew rapidly with electron density n . These observations are consistent with the fact that the exchange constant J given by Eq. (3) is exponentially small at $n_B \ll 1$.

Acknowledgments

The authors are grateful to L. I. Glazman and B. I. Halperin for stimulating discussions. Work at Argonne National Laboratory was supported by the U.S. Department of Energy, Office of Science, Materials Sciences and Engineering Division. Work at the University of Washington was supported by U. S. Department of Energy Office of Science, Basic Energy Sciences under award number DE-FG02-07ER46452.

Appendix A: Evaluation of phonon frequencies in the Wigner crystal at low wavenumber

The frequencies of phonons in a one-dimensional Wigner crystal are given by Eq. (12). Upon the introduction of the dimensionless time τ via Eq. (21), the phonon frequencies become

$$\omega_q^2 = 4 \sum_{l=1}^{\infty} \frac{1}{l^3} [1 - \cos(ql)]. \quad (A1)$$

At $q \rightarrow 0$ one can expand the cosine and obtain the logarithmic behavior

$$\omega_q^2 = 2q^2 \ln \frac{\chi}{q}. \quad (A2)$$

A more careful calculation is required to obtain the value of the constant χ , which is the subject of this Appendix.

We start by substituting the identity

$$\frac{1}{l^3} = \frac{1}{2} \int_0^{\infty} x^2 e^{-lx} dx$$

into Eq. (A1) and performing the trivial summation over l in the resulting expression:

$$\omega_q^2 = \int_0^{\infty} x^2 \left[\frac{2}{e^x - 1} - \frac{1}{e^{x+iq} - 1} - \frac{1}{e^{x-iq} - 1} \right] dx. \quad (A3)$$

Let us now split the above integral into two, with the first one taken from 0 to x_0 and the second from x_0 to ∞ . The value of x_0 is chosen such that $q \ll x_0 \ll 1$. In the first integral one can expand $e^x \simeq 1 + x$ and obtain

$$\int_0^{x_0} x^2 \left[\frac{2}{e^x - 1} - \frac{1}{e^{x+iq} - 1} - \frac{1}{e^{x-iq} - 1} \right] dx \\ \simeq 2q^2 \int_0^{x_0} \frac{x dx}{x^2 + q^2} \simeq 2q^2 \ln \frac{x_0}{q}.$$

To evaluate the second integral we expand the integrand to second order in small q and obtain

$$\int_{x_0}^{\infty} x^2 \left[\frac{2}{e^x - 1} - \frac{1}{e^{x+iq} - 1} - \frac{1}{e^{x-iq} - 1} \right] dx \\ \simeq \int_{x_0}^{\infty} x^2 q^2 \left(\frac{1}{e^x - 1} \right)'' dx \simeq q^2 [-2 \ln x_0 + 3].$$

The total integral in Eq. (A3) is independent of x_0 and given by

$$\omega_q^2 = 2q^2 \ln \frac{1}{q} + 3q^2.$$

Comparing this result with Eq. (A2) we obtain $\chi = e^{3/2} \approx 4.48$.

Appendix B: Analytical treatment of the instanton action

The instanton action (23) is minimized for the configuration in which the electrons rest at the positions of static equilibrium $X_l(\tau) = l$. Small fluctuations near the minimum can be studied by introducing the displacements u_l of electrons from equilibrium positions

$$X_l(\tau) = l + u_l(\tau). \quad (\text{B1})$$

Substituting Eq. (B1) into (23) and expanding in u_l one finds the quadratic action

$$\eta^{(2)} = \int_{-\infty}^{\infty} \left(\sum_l \frac{1}{2} \dot{u}_l^2 + \sum_{l < l'} \frac{(u_{l'} - u_l)^2}{(l' - l)^3} \right) d\tau. \quad (\text{B2})$$

Upon the Fourier transformation of the displacements

$$u_l(\tau) = \int \frac{dq d\omega}{(2\pi)^2} e^{iql - i\omega\tau} u_{q\omega} \quad (\text{B3})$$

the quadratic action takes the form

$$\eta^{(2)} = \int \frac{dq d\omega}{(2\pi)^2} \frac{1}{2} (\omega^2 + \omega_q^2) |u_{q\omega}|^2. \quad (\text{B4})$$

The phonon frequencies ω_q are evaluated in Appendix A.

1. Single instanton

The amplitude of the nearest-neighbor exchange between sites 0 and 1 is determined by the action of an instanton with the boundary conditions $X_0(-\infty) = X_1(+\infty) = 0$, $X_0(+\infty) = X_1(-\infty) = 1$, and $X_l(\pm\infty) = l$ for all $l \neq 0, 1$. Minimization of Eq. (23) over all $X_l(\tau)$ then results in the single-instanton action $\eta \approx 2.80$.⁷

It is instructive to study interaction of the instanton with long-wavelength fluctuations of the displacements $u_l(\tau)$. A shift of all u_l by a constant δu corresponds to the translation of the whole crystal and has no effect on the action. A uniform $\dot{u}_l = v$ has the meaning of the velocity of the crystal. Although the instanton action is affected by the motion of the system as a whole, the effect should be even in v , and thus instanton action does not couple to \dot{u}_l in first order. On the other hand, the spatial derivative $\partial_l u$ corresponds to stretching the crystal and results in the change of density

$$n = \frac{n_0}{1 + \partial_l u}. \quad (\text{B5})$$

Since the dimensionless action (23) assumes that density equals 1, the effect of the change $n_0 \rightarrow n$ should be obtained from the full expression (22). Substituting Eq. (B5) one then obtains

$$\frac{1}{\hbar} S_1 = \frac{\eta}{\sqrt{n_0 a_B}} \sqrt{1 + \partial_l u} \simeq \frac{1}{\sqrt{n_0 a_B}} \left(\eta + \frac{\eta}{2} \partial_l u \right).$$

Thus to lowest order the instanton couples linearly to fluctuations of the field $u_l(\tau)$,

$$\delta\eta = d \partial_l u, \quad d = \frac{\eta}{2}, \quad (\text{B6})$$

where the derivative $\partial_l u$ is taken at l and τ corresponding to the location of the instanton.

2. Interaction of instantons

Let us now consider the configuration of $X_l(\tau)$ corresponding to two instantons at positions $(0, 0)$ and (l, τ) . Assuming the instantons are far from each other, $l^2 + \tau^2 \gg 1$, the action can be presented as

$$\eta_2(l, \tau) = 2\eta + \delta\eta(l, \tau), \quad (\text{B7})$$

where the small correction $\delta\eta(l, \tau)$ has the meaning of the interaction between the instantons. To find it one can minimize the quadratic action (B2) with the perturbation $d[\partial_l u(0, 0) + \partial_l u(l, \tau)]$. An alternative approach is to find the shape $u(l, \tau)$ of the instanton centered at $(0, 0)$ at large distance using the perturbation $d\partial_l u(0, 0)$ and then apply Eq. (B6) to find coupling to the second instanton. Following this approach one easily obtains

$$u(l, \tau) = d \int \frac{dq d\omega}{(2\pi)^2} \frac{i q e^{iq l - i\omega\tau}}{\omega^2 + \omega_q^2} \quad (\text{B8})$$

at large distances from the first instanton. The interaction of the instantons is obtained by differentiating the above expression:

$$\begin{aligned}\delta\eta(l, \tau) &= -d^2 \int \frac{dq d\omega}{(2\pi)^2} \frac{q^2 e^{iql-i\omega\tau}}{\omega^2 + \omega_q^2} \\ &= -d^2 \int \frac{dq}{4\pi} \frac{q^2}{\omega_q} e^{iql-\omega_q|\tau|}.\end{aligned}\quad (\text{B9})$$

3. Electrostatic analogy

Because of the logarithmic singularity in ω_q , see Eq. (A2), the remaining integral in Eq. (B9) cannot be easily performed. On the other hand, considerable progress can be made by replacing $\ln(\chi/q)$ with a constant, $\omega_q \simeq sq$. Using this approximation, we immediately find

$$\delta\eta(l, \tau) = \frac{d^2}{2\pi s} \frac{l^2 - s^2\tau^2}{(l^2 + s^2\tau^2)^2}.\quad (\text{B10})$$

This result has the form of interaction of two dipoles in two-dimensional space $(l, s\tau)$.

The analogy is developed as follows. The action (B2) is presented as

$$\eta_{el} = \int d^2r \left[\frac{s}{2} (\nabla u)^2 - \rho u \right],\quad (\text{B11})$$

where we have added the “charge density” term ρu . Minimization of η_{el} with respect to u gives the Poisson equation $\nabla^2 u = -\rho/s$, with s playing the role of ε_0 in SI units. Substitution of $\rho = -s\nabla^2 u$ into Eq. (B11) enables one to express the action in terms of the “electric potential” u ,

$$\eta_{el} = - \int d^2r \frac{s}{2} (\nabla u)^2.\quad (\text{B12})$$

Thus the action η_{el} is given by the energy of the effective electric field with the opposite sign.

The coupling term (B6) corresponds to $\rho = d\partial_l\delta(\mathbf{r})$, analogous to the charge distribution in a dipole pointing in the l direction. In two dimensions, the interaction between two such dipoles is given by the negative of Eq. (B10), as expected in our electrostatic analogy.

-
- ¹ T. Giamarchi, *Quantum Physics in One Dimension* (Clarendon Press, Oxford, 2004).
 - ² I. E. Dzyaloshinskii and A. I. Larkin, Sov. Phys. JETP **38**, 202 (1974).
 - ³ M. Ogata and H. Shiba, Phys. Rev. B **41**, 2326 (1990).
 - ⁴ K.-F. Berggren and M. Pepper, Physics World **15**, 37 (2002).
 - ⁵ E. Wigner, Phys. Rev. **46**, 1002 (1934).
 - ⁶ K. A. Matveev, Phys. Rev. B **70**, 245319 (2004).
 - ⁷ A. D. Klironomos, R. R. Ramazashvili, and K. A. Matveev, Phys. Rev. B **72**, 195343 (2005).
 - ⁸ M. M. Fogler and E. Pivovarov, Phys. Rev. B **72**, 195344 (2005).
 - ⁹ H. Bethe, Z. Physik **71**, 205 (1931).
 - ¹⁰ T. Micklitz, J. Rech, and K. A. Matveev, Phys. Rev. B **81**, 115313 (2010).
 - ¹¹ A. Levchenko, T. Micklitz, J. Rech, and K. A. Matveev, Phys. Rev. B **82**, 115413 (2010).
 - ¹² A. V. Andreev, S. A. Kivelson, and B. Spivak, Phys. Rev. Lett. **106**, 256804 (2011).
 - ¹³ K. A. Matveev and A. V. Andreev, Phys. Rev. Lett. **107**, 056402 (2011).
 - ¹⁴ A. Levchenko, T. Micklitz, Z. Ristivojevic, and K. A. Matveev, Phys. Rev. B **84**, 115447 (2011).
 - ¹⁵ A. P. Dmitriev, I. V. Gornyi, and D. G. Polyakov, Phys. Rev. B **86**, 245402 (2012).
 - ¹⁶ S. Apostolov, D. E. Liu, Z. Maizelis, and A. Levchenko, Phys. Rev. B **88**, 045435 (2013).
 - ¹⁷ K. A. Matveev, A. V. Andreev, and M. Pustilnik, Phys. Rev. Lett. **105**, 046401 (2010).
 - ¹⁸ K. A. Matveev and A. V. Andreev, Phys. Rev. B **85**, 041102 (2012).
 - ¹⁹ K. A. Matveev and A. V. Andreev, Phys. Rev. B **86**, 045136 (2012).
 - ²⁰ A. D. Klironomos, J. S. Meyer, and K. A. Matveev, Europhys. Lett. **74**, 679 (2006).
 - ²¹ A. D. Klironomos, J. S. Meyer, T. Hikihara, and K. A. Matveev, Phys. Rev. B **76**, 075302 (2007).
 - ²² D. J. Thouless, Proc. Phys. Soc. **86**, 893 (1965).
 - ²³ K. A. Matveev, J. Exp. Theor. Phys. **117**, 508 (2013).
 - ²⁴ J. des Cloizeaux and J. J. Pearson, Phys. Rev. **128**, 2131 (1962).
 - ²⁵ L. Faddeev and L. Takhtajan, Phys. Lett. A **85**, 375 (1981).
 - ²⁶ F. D. M. Haldane, J. Phys. C: Solid State Phys. **14**, 2585 (1981).
 - ²⁷ A. Lamacraft, Phys. Rev. Lett. **101**, 225301 (2008).
 - ²⁸ P. Nozières and A. Blandin, J. Phys. (Paris) **41**, 193 (1980).
 - ²⁹ A. H. Castro Neto and M. P. A. Fisher, Phys. Rev. B **53**, 9713 (1996).
 - ³⁰ E. M. Lifshitz and L. P. Pitaevskii, *Physical Kinetics* (Butterworth-Heinemann, Oxford, 1981).
 - ³¹ T. L. Schmidt, A. Imambekov, and L. I. Glazman, Phys. Rev. B **82**, 245104 (2010).
 - ³² T. Karzig, L. I. Glazman, and F. von Oppen, Phys. Rev. Lett. **105**, 226407 (2010).
 - ³³ M.-T. Rieder, T. Micklitz, and A. Levchenko, unpublished.
 - ³⁴ A. Kristensen, H. Bruus, A. E. Hansen, J. B. Jensen, P. E. Lindelof, C. J. Marckmann, J. Nygård, C. B. Sørensen, F. Beuscher, A. Forchel, and M. Michel, Phys. Rev. B **62**, 10950 (2000).
 - ³⁵ M. Andrews, Am. J. Phys. **44**, 1064 (1976).
 - ³⁶ Strictly speaking, the one-dimensional Coulomb barrier is impenetrable.³⁵ On the other hand, quantum wires always have finite width w , which results in finite tunneling amplitude depending only logarithmically on w , see Ref. 8.

